

Supporting information

Porphyrin-based photosensitizers for visible-light polymerization and antibacterial applications

Fanny Schnetz,^a Iryna Knysh,^b Denis Jacquemin,^{b,c} Samir Abbad Andaloussi,^d Marc Presset,^a Sonia Lajnef,^e Fabienne Peyrot,^{e,f} Davy-Louis Versace^{*a}

^a*Univ Paris Est Créteil, CNRS, ICMPE, UMR 7182, 2 rue Henri Dunant, 94320 Thiais, France.*

^b*Nantes Université, CNRS, CEISAM UMR 6230, F-44000 Nantes, France.*

^c*Institut Universitaire de France, F-75005 Paris, France.*

^d*Laboratoire Eau, Environnement, Systèmes Urbains (LEESU), Université Paris-Est (UPEC), UMR-MA 102, 61 Avenue Général de Gaulle, Créteil 94010, France.*

^e*Université Paris Cité, CNRS, Laboratoire de Chimie et Biochimie Pharmacologiques et Toxicologiques, F-75006 Paris, France.*

^f*Sorbonne Université, Institut National Supérieur du Professorat et de l'Éducation de l'Académie de Paris, F-75016 Paris, France.*

Figure S1: ^1H NMR spectrum of PBP in CDCl_3 .	S4
Figure S2: ^{13}C NMR spectrum of PBP in CDCl_3 .	S4
Figure S3: ^1H NMR spectrum of PBPZn in CDCl_3 .	S5
Figure S4: ^{13}C NMR spectrum of PBPZn in CDCl_3 .	S5
Figure S5: Absorption spectra of PBP and PBPZn associated with the emission spectra of the LEDs used in this study (LEDs@385, 405, 455 and 530 nm).	S6
Figure S6: Optimal ground-state structures of PBP (left) and PBPZn (right).	S6
Figure S7: Vibrationally-resolved spectrum of PBP simulated using the Vertical Hessian model and internal coordinates.	S7
Figure S8: Vibrationally-resolved spectrum of PBP simulated using the Vertical Hessian model and Cartesian coordinates. The imaginary frequency for the excited states were turned real (one such frequency for S1, S2, and S4).	S7
Figure S9: Vibrationally-resolved spectrum of PBPZn simulated using the Vertical Hessian model and Cartesian coordinates. Note that for both S1 and S4, imaginary frequencies exist in the excited-state (vertical) Hessian, and they have been turned positive.	S8
Figure S10: Vertical transition energies, associated oscillator strengths and electron density difference plots for PBP . In the latter representations, the blue and red lobes correspond to decrease and increase of density upon absorption (threshold 0.005 au).	S8
Figure S11: Vertical transition energies, associated oscillator strengths and electron density difference plots for PBPZn . See previous caption for more details.	S9
Figure S12: Transition absorption spectra of PBP and PBPZn under argon in DCM ($\lambda_{\text{exc}} = 385 \text{ nm}$).	S10
Figure S13: Decay traces of the triplet excited state of A) PBP and B) PBPZn after a laser pulse ($\lambda_{\text{ex}} = 385 \text{ nm}$) with and without oxygen in DCM.	S10
Figure S14: Photolysis of A) PBP and B) PBPZn solution under LED@405 nm irradiation. [PBP] = $2 \times 10^{-6} \text{ mol.L}^{-1}$, [PBPZn] = $6 \times 10^{-6} \text{ mol.L}^{-1}$, [MDEA] = $2.8 \times 10^{-2} \text{ mol.L}^{-1}$. Solvent = DCM.	S11
Figure S15: The normalized experimental (1) and simulated (2) EPR spectra obtained upon continuous in situ LED@400 nm exposure in chloroform under irradiation for (A) PBPZn , (B) PBP with DMPO and (C) PBPZn with DMPO.	S12
Figure S16 : Steady state photolysis of A) PBP /MDEA and B) PBPZn /MDEA systems under air after LED@405 nm exposure. [PBP] = $2 \times 10^{-6} \text{ mol.L}^{-1}$, [PBPZn] = $6 \times 10^{-6} \text{ mol.L}^{-1}$, [MDEA] = $2.8 \times 10^{-2} \text{ mol.L}^{-1}$. Solvent = DCM.	S13
Figure S17 : Quenching of A) PBP and B) PBPZn fluorescence after a gradual addition of MDEA. [PBP] = $1.2 \times 10^{-7} \text{ mol.L}^{-1}$, [PBPZn] = $5.2 \times 10^{-6} \text{ mol.L}^{-1}$ (solvent: THF). Corresponding Stern-Volmer plot for the quenching of the singlet excited state of C) PBP ($K_{\text{SV}}^{\text{PBP/MDEA}} = 1.2 \text{ M}^{-1}$) and D) PBPZn ($K_{\text{SV}}^{\text{PBPZn/MDEA}} = 0.7 \text{ M}^{-1}$) with MDEA.	S13
Figure S18 : Decay traces of A) PBP and B) PBPZn triplet excited state after a laser pulse ($\lambda_{\text{ex}} = 385 \text{ nm}$) with a gradual addition of MDEA. C) Corresponding Stern-Volmer plot for the quenching of the triplet excited state of PBP with MDEA. [PBP] = $1.1 \times 10^{-5} \text{ mol.L}^{-1}$, [PBPZn] = $1.7 \times 10^{-4} \text{ mol.L}^{-1}$, [MDEA] = 8.7 mol.L^{-1} in DCM.	S14
Figure S19: The normalized experimental (1) and simulated (2) EPR spectra obtained upon continuous in situ LED@400 nm exposure of PBPZn /MDEA in chloroform and under argon.	S14
Figure S20 : The normalized experimental (1) and simulated (2) EPR spectra obtained upon continuous in situ LED@400 nm exposure of porphyrin derivatives in chloroform under argon in the presence DMPO spin trapping agent and MDEA for A) PBP and B) PBPZn .	S15
Figure S21: Steady state photolysis of A) PBP /Iod and B) PBPZn /Iod systems under air after LED@405 nm exposure. [PBP] = $2 \times 10^{-6} \text{ mol.L}^{-1}$, [PBPZn] = $6 \times 10^{-6} \text{ mol.L}^{-1}$, [Iod] = $2.9 \times 10^{-5} \text{ mol.L}^{-1}$. Solvent = DCM.	S15
Figure S22: Quenching of A) PBP and B) PBPZn fluorescence after a gradual addition of Iod. [PBP] = $1.2 \times 10^{-7} \text{ mol.L}^{-1}$, [PBPZn] = $5.2 \times 10^{-6} \text{ mol.L}^{-1}$ (solvent = THF). Corresponding Stern-Volmer plot for the quenching of the singlet excited state of C) PBP ($K_{\text{SV}}^{\text{PBP/Iod}} = 11 \text{ M}^{-1}$) and D) PBPZn ($K_{\text{SV}}^{\text{PBPZn/Iod}} = 13 \text{ M}^{-1}$) with the addition of Iod.	S16
Figure S23: Decay traces of A) PBP and B) PBPZn triplet state after a laser pulse ($\lambda_{\text{ex}} = 385 \text{ nm}$) with a gradual addition of Iod. Corresponding Stern-Volmer plot for the quenching of the triplet excited state of C) PBP and D) PBPZn with the addition of Iod. [PBP] = $1.1 \times 10^{-5} \text{ mol.L}^{-1}$, [PBPZn] = $1.7 \times 10^{-4} \text{ mol.L}^{-1}$ in DCM.	S17
Figure S24: The normalized experimental (1) and simulated (2) EPR spectra obtained post 120-s LED@405 nm exposure of (A) PBP and (B) PBPZn . in chloroform under argon in the presence DMPO spin trapping agent and Iod. (* denote the	

artefactual triplet lines resulting from double addition of MePh radical on DMPO following a mechanism similar to that detailed in Figure S32 with thiyl radicals).....	S17
Figure S25: Steady-state photolysis of A) PBP/Iod/rhodamine B and B) PBPZn/Iod/rhodamine B after irradiation by LED@405 nm under air conditions. Absorbance increase at 570 nm along time for C) PBP and D) PBPZn . [PBP] = 2×10^{-6} mol.L ⁻¹ , [PBPZn] = 6×10^{-6} mol.L ⁻¹ , [Iod] = 2.9×10^{-5} mol.L ⁻¹ , [RhB] = 2.4×10^{-5} mol.L ⁻¹	S18
Figure S26: The normalized experimental (1) and simulated (2) EPR spectra obtained upon continuous in situ LED@400 nm exposure of (A) PBP and (B) PBPZn in chloroform and under argon in the presence DMPO spin trapping agent and cysteamine: × denotes the broad signal assigned to PBPZn ^{•-}	S19
Figure S27: Quenching of A) PBP and B) PBPZn fluorescence after a gradual addition of cysteamine. [PBP] = 1.2×10^{-7} mol.L ⁻¹ , [PBPZn] = 5.2×10^{-6} mol.L ⁻¹ (solvent = THF). Corresponding Stern-Volmer plot for the quenching of the singlet excited state of C) PBP ($K_{SV}^{PBP/cysteamine} = 1.2 \text{ M}^{-1}$) and D) PBPZn ($K_{SV}^{PBPZn/cysteamine} = 6.2 \text{ M}^{-1}$).....	S19
Figure S28: Decay traces of A) PBP and B) PBPZn triplet state after a laser pulse ($\lambda_{ex} = 385 \text{ nm}$) with a gradual increase of the cysteamine concentration. [PBP] = 1.1×10^{-5} mol.L ⁻¹ , [PBPZn] = 1.7×10^{-4} mol.L ⁻¹ in DCM.	S20
Figure S29: Steady state photolysis of A) PBP/N-acetylcysteine and B) PBPZn/N-acetylcysteine systems under air after LED@405 nm exposure. [PBP] = 2×10^{-6} mol.L ⁻¹ , [PBPZn] = 6×10^{-6} mol.L ⁻¹ , [N-acetylcysteine] = 1.1×10^{-4} mol.L ⁻¹ . Solvent = DCM.	S20
Figure S30: Decay traces of A) PBP and B) PBPZn triplet state after laser pulses ($\lambda_{ex} = 385 \text{ nm}$) with a gradual addition of N-acetylcysteine. Corresponding Stern-Volmer plot for the quenching of the triplet excited state of C) PBP with N-acetylcysteine. [PBP] = 1.1×10^{-5} mol.L ⁻¹ , [PBPZn] = 1.7×10^{-4} mol.L ⁻¹ in DCM.....	S21
Figure S31: The normalized experimental (1) and simulated (2) EPR spectra obtained upon continuous in situ LED@405 nm exposure of (A) PBP and (B) PBPZn in chloroform and under argon in the presence of DMPO spin trapping agent and N-acetylcysteine.	S21
Figure S32: A) Dismutation reaction between two DMPO-SR adduct a leading to the formation of hydroxylamine b and nitron c by redox reaction. B) Reaction between nitron c and thiyl radical leading to nitroxide d	S22
Figure S33: Forrester-Hepburn mechanism	S22
Figure S34: Polymerization profiles (acrylate function conversion vs. irradiation time) for SOA in laminate (solid line) and under air (dash line) in the presence of 1) BP/MDEA (0.5%/2% w/w), 2) BP/Iod (0.5%/2% w/w), 3) BP/cysteamine (0.5%/1% w/w), 4) BP/N-acetylcysteine (0.5%/2% w/w) upon irradiation of (a) LED@385 nm in laminate, (b) LED@385 nm under air, (c) LED@405 nm in laminate, (d) LED@405 nm under air, (e) LED@505 nm under air and (f) LED@530 nm in laminate.	S22
Figure S35: Polymerization profiles (acrylate function conversion vs. irradiation time) for SOA in laminate (solid line) and under air (dash line) in the presence of 1) CQ/MDEA (0.5%/2% w/w), 2) CQ/Iod (0.5%/2% w/w), 3) BP/N-acetylcysteine (0.5%/2% w/w) upon irradiation with (a) LED@385 nm in laminate, (b) LED@385 nm under air, (c) LED@405 nm in laminate, (d) LED@405 nm under air, (e) LED@505 nm in laminate, (d) LED@505 nm under air, (f) LED@530 nm in laminate and (g) LED@530 nm under air.....	S23
Figure S36: Polymerization profiles (acrylate conversion vs. irradiation time) for SOA in laminate (solid line) and under air (dash line) in the presence of 1) PBP/MDEA (0.5%/2% w/w), 2) PBP/Iod (0.5%/2% w/w), 3) PBP/cysteamine (0.5%/1% w/w) and 4) PBP/N-acetylcysteine (0.5%/2% w/w) upon irradiation with (a) LED@385 nm in laminate, (b) LED@385 nm under air, (c) LED@405 nm in laminate, (d) LED@405 nm under air, (e) LED@505 nm in laminate, (d) LED@505 nm under air, (f) LED@530 nm in laminate and (g) LED@530 nm under air.	S23
Figure S37: Polymerization profiles (acrylate function conversion vs. irradiation time) for SOA in laminate (solid line) and under air (dash line) in the presence of 1) PBPZn/MDEA (0.5%/2% w/w), 2) PBPZn/Iod (0.5%/2% w/w), 3) PBPZn/cysteamine (0.5%/1% w/w) and 4) PBPZn/N-acetylcysteine (0.5%/2% w/w) upon irradiation with (a) LED@385 nm in laminate, (b) LED@385 nm under air, (c) LED@405 nm in laminate, (d) LED@405 nm under air, (e) LED@505 nm in laminate, (d) LED@505 nm under air, (f) LED@530 nm in laminate and (g) LED@530 nm under air.	S24
Figure S38: Optical image of the PBPZn -based pellet	S24

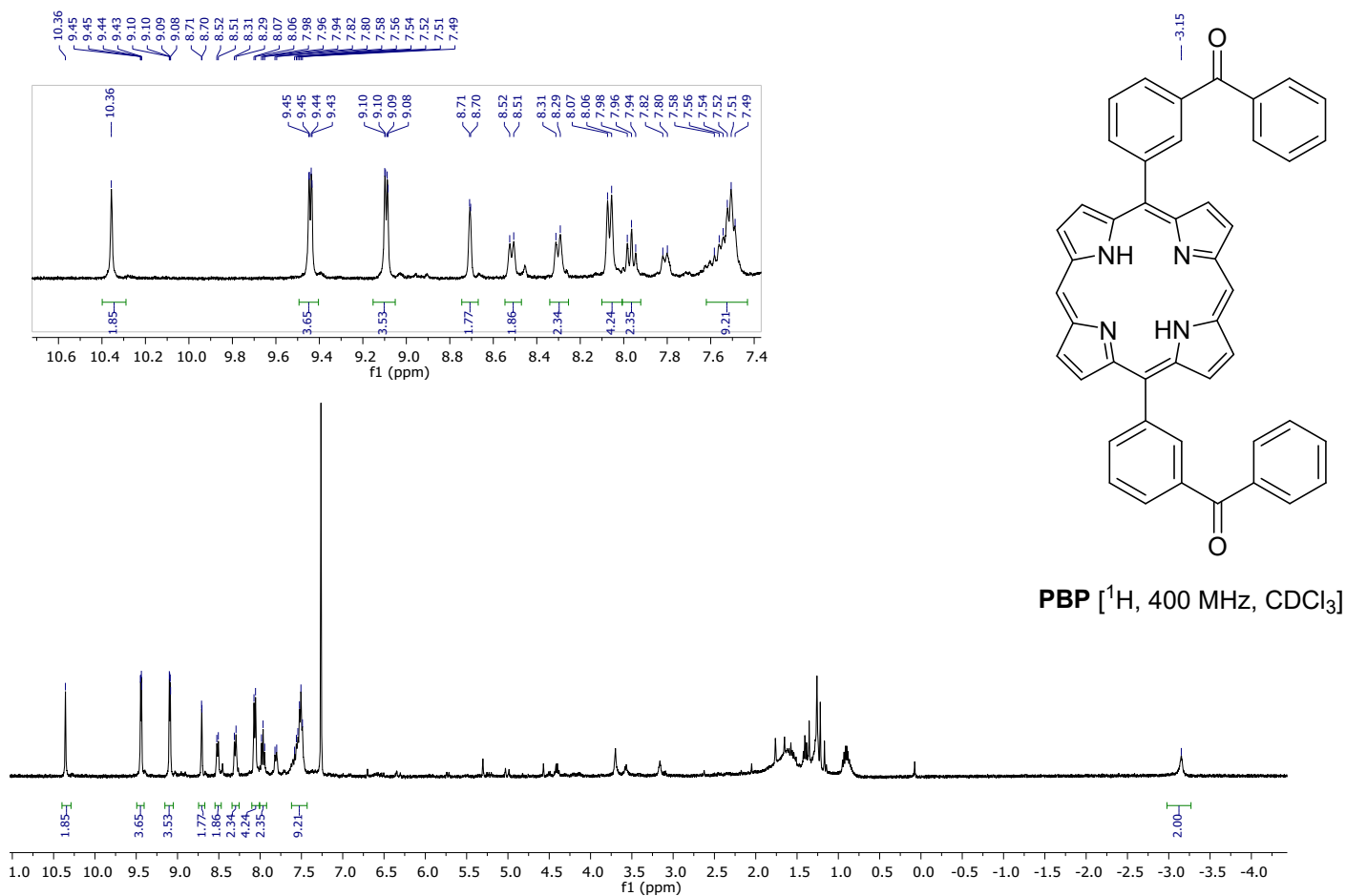


Figure S1: ^1H NMR spectrum of PBP in CDCl_3 .

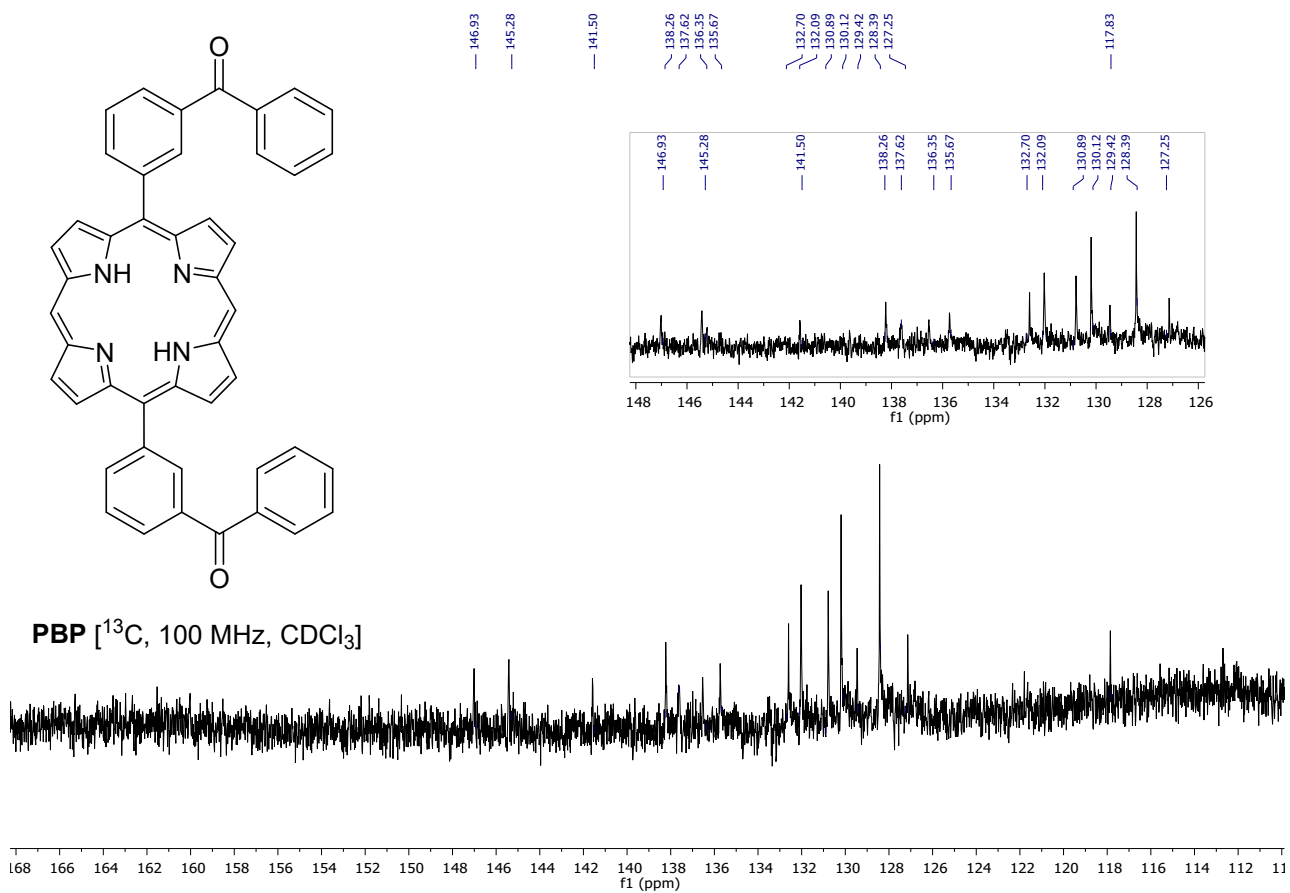


Figure S2: ^{13}C NMR spectrum of PBP in CDCl_3 .

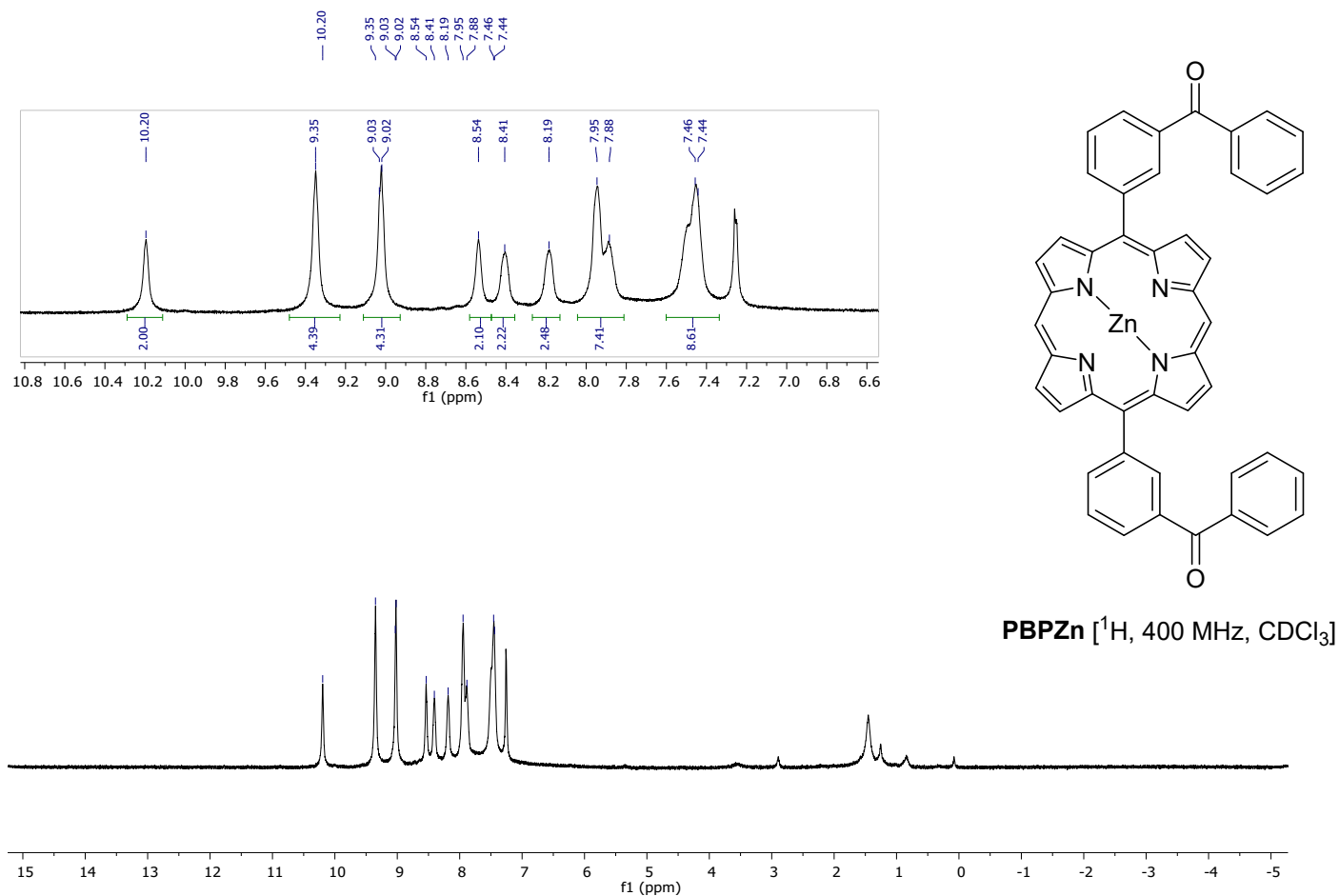


Figure S3: ^1H NMR spectrum of **PBPZn** in CDCl_3 .

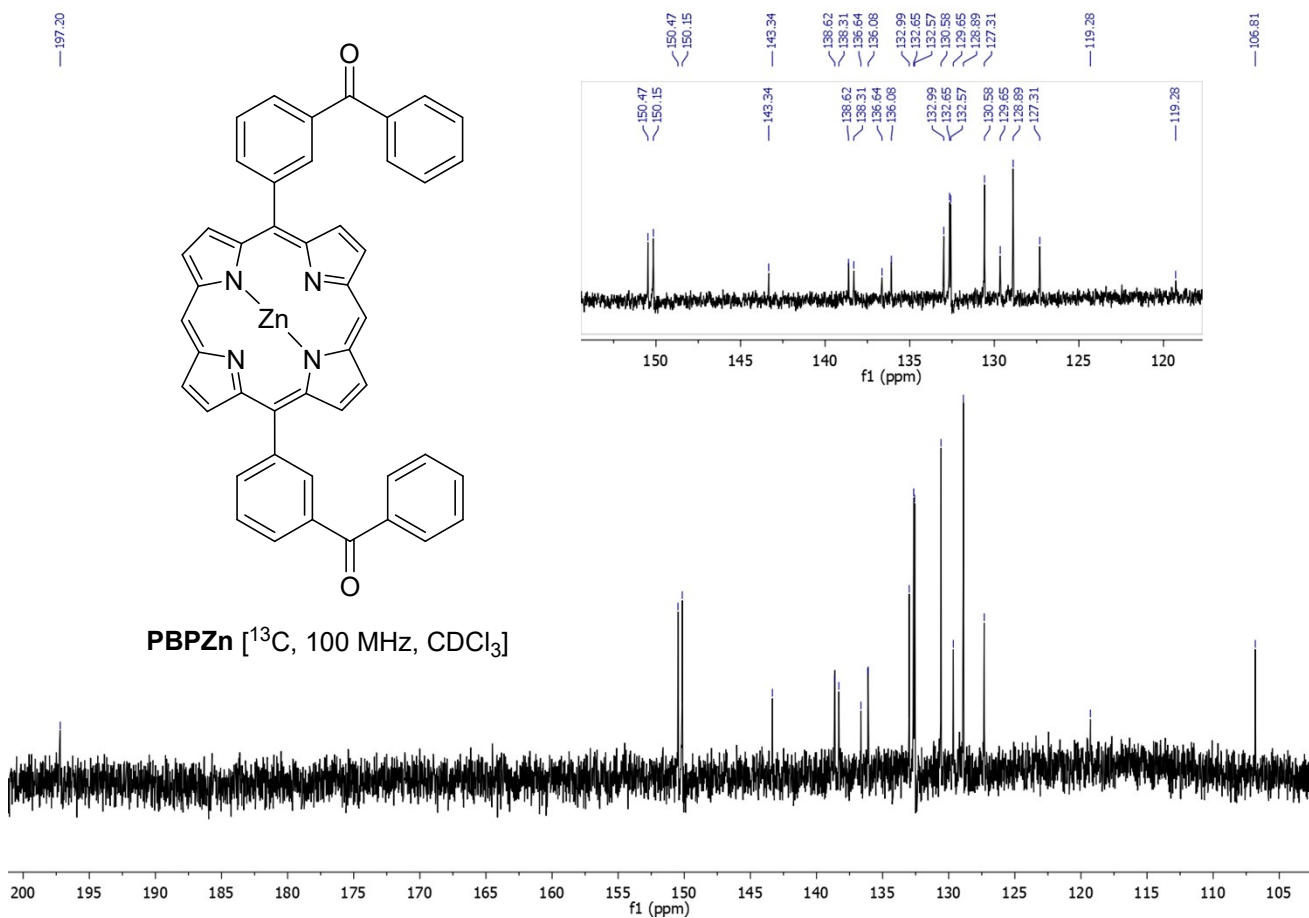


Figure S4: ^{13}C NMR spectrum of **PBPZn** in CDCl_3 .

Absorption

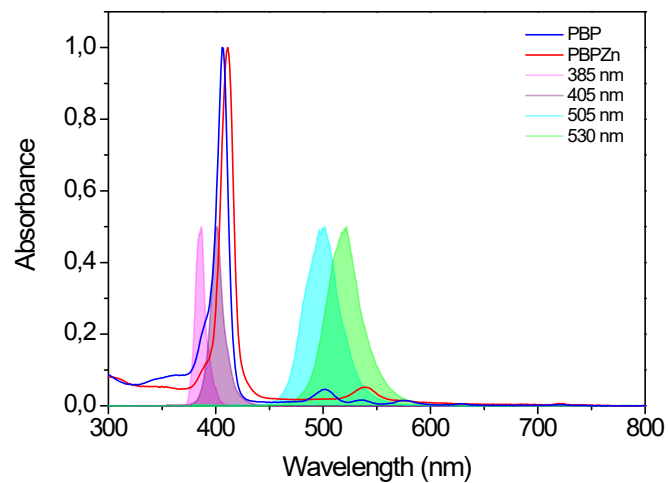


Figure S5: Absorption spectra of **PBP** and **PBPZn** associated with the emission spectra of the LEDs used in this study (LEDs@385, 405, 455 and 530 nm).

TD-DFT calculations



Figure S6: Optimal ground-state structures of **PBP** (left) and **PBPZn** (right).

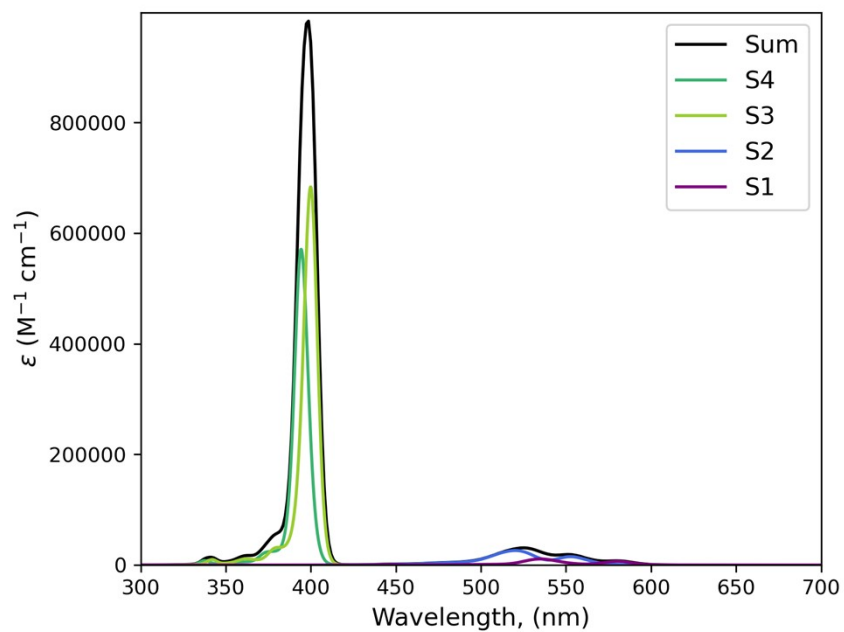


Figure S7: Vibrationally-resolved spectrum of **PBP** simulated using the Vertical Hessian model and internal coordinates.

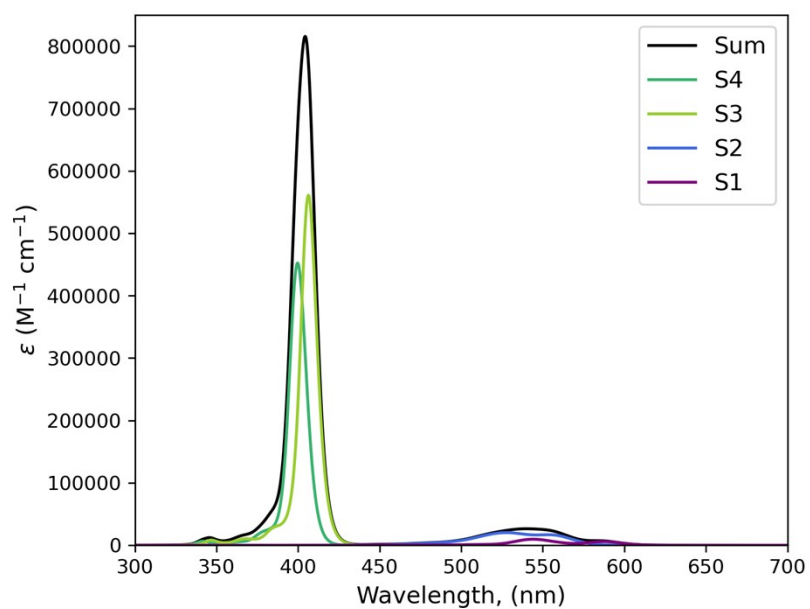


Figure S8: Vibrationally-resolved spectrum of **PBP** simulated using the Vertical Hessian model and Cartesian coordinates. The imaginary frequency for the excited states were turned real (one such frequency for S1, S2, and S4)

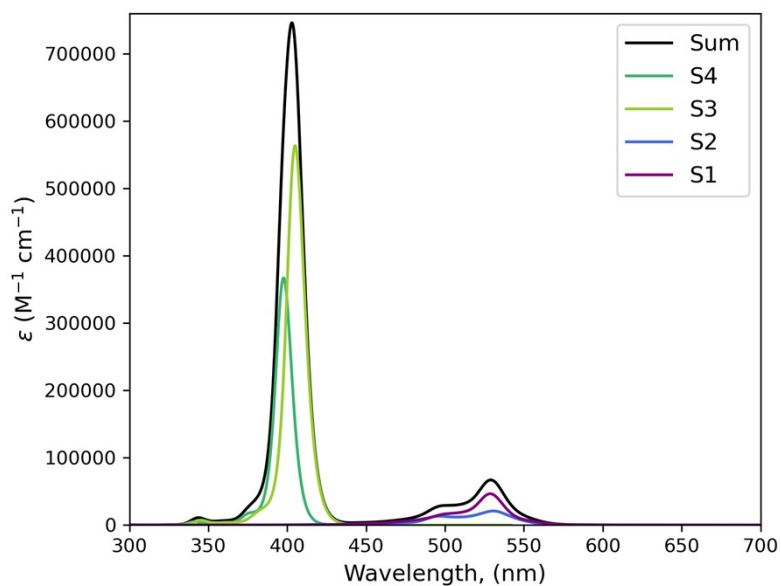


Figure S9: *Vibrationally-resolved spectrum of PBPZn simulated using the Vertical Hessian model and Cartesian coordinates. Note that for both S1 and S4, imaginary frequencies exist in the excited-state (vertical) Hessian, and they have been turned positive.*

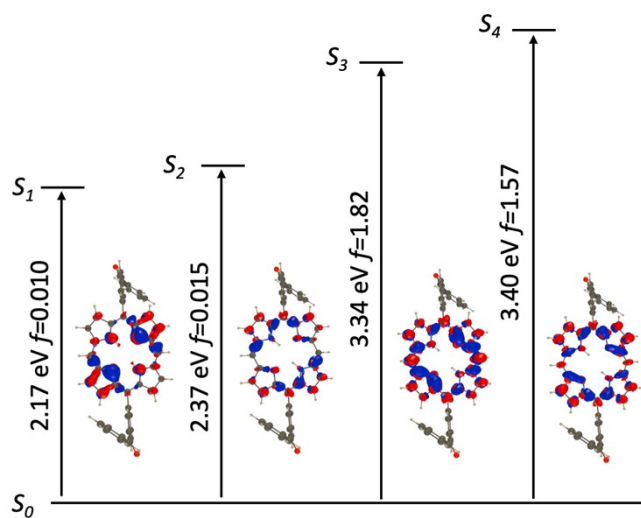


Figure S10: *Vertical transition energies, associated oscillator strengths and electron density difference plots for PBP. In the latter representations, the blue and red lobes correspond to decrease and increase of density upon absorption (threshold 0.005 au).*

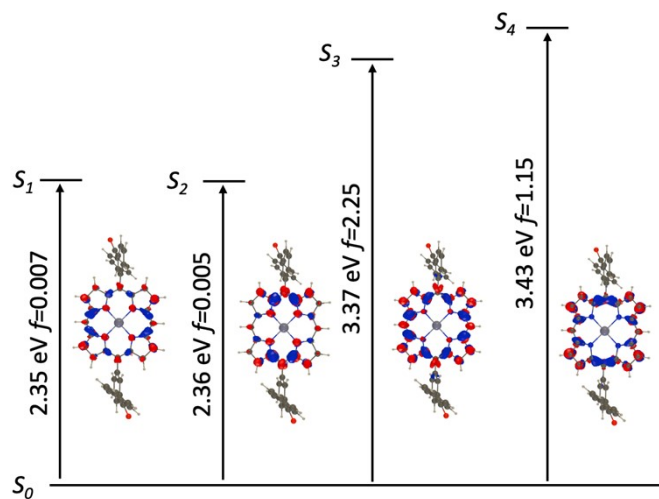


Figure S11: Vertical transition energies, associated oscillator strengths and electron density difference plots for **PBPZn**. See previous caption for more details.

Absorption & emission

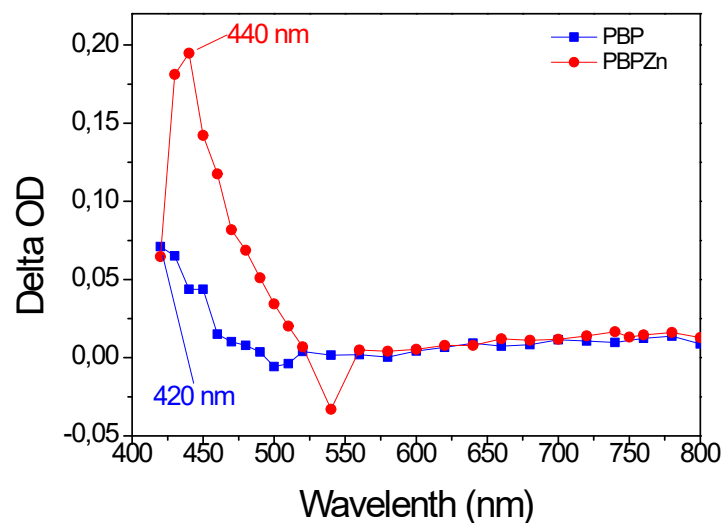


Figure S12: Transition absorption spectra of *PBP* and *PBPZn* under argon in DCM ($\lambda_{exc} = 385$ nm)

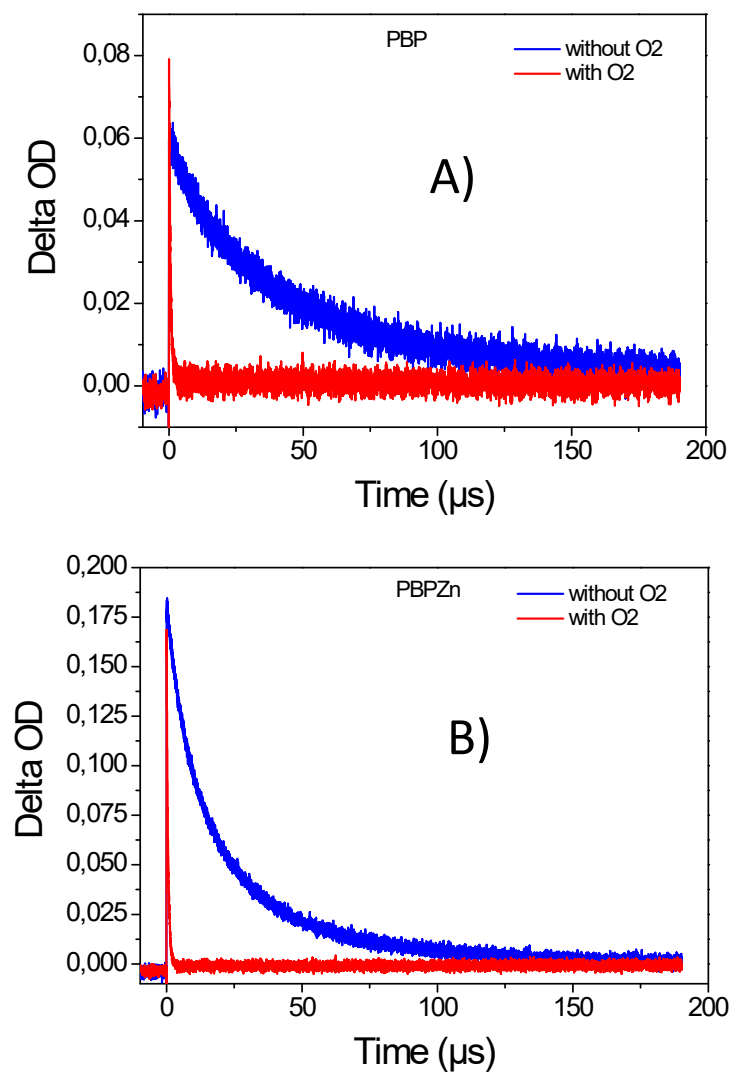


Figure S13: Decay traces of the triplet excited state of A) *PBP* and B) *PBPZn* after a laser pulse ($\lambda_{ex} = 385$ nm) with and without oxygen in DCM.

Cyclic voltammetry

Table S1: Redox values and photophysical properties of the photoinitiating compounds

Molecules	E _{ox} (eV)	E _{red} (eV)	E _S (eV)	E _T (eV)
PBP	1.47	-1.18	2.03	2.95
PBPZn	1.09	-1.48	2.14	2.82
BP	0.16	-1.20		2.38
CQ	0.12	-1.25		2.21
MDEA	0.72		-	-
Iod	-	-0.63	-	-
cysteamine	0.92		-	-
N-acetylcysteine	0.79		-	-

Photostability of the porphyrin derivatives

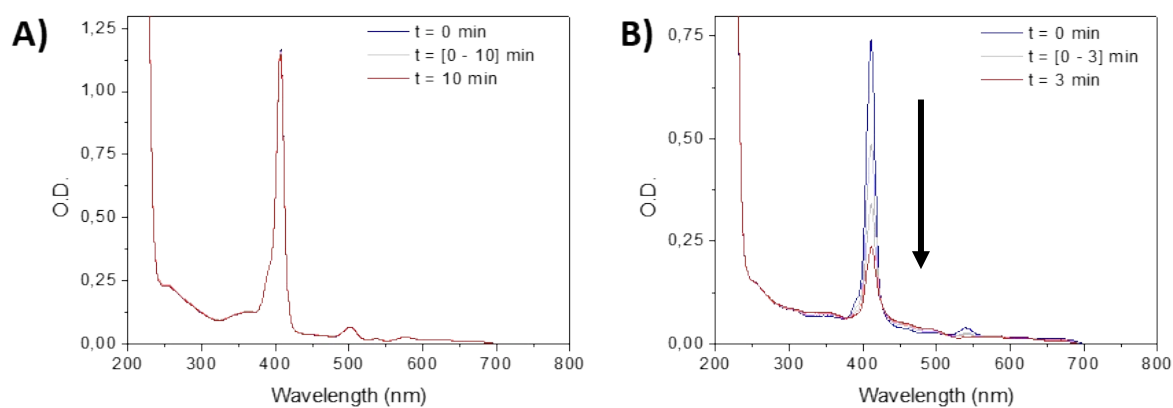


Figure S14: Photolysis of **A) PBP** and **B) PBPZn** solution under LED@405 nm irradiation. $[PBP] = 2 \times 10^{-6} \text{ mol.L}^{-1}$, $[PBPZn] = 6 \times 10^{-6} \text{ mol.L}^{-1}$, $[MDEA] = 2.8 \times 10^{-2} \text{ mol.L}^{-1}$. Solvent = DCM.

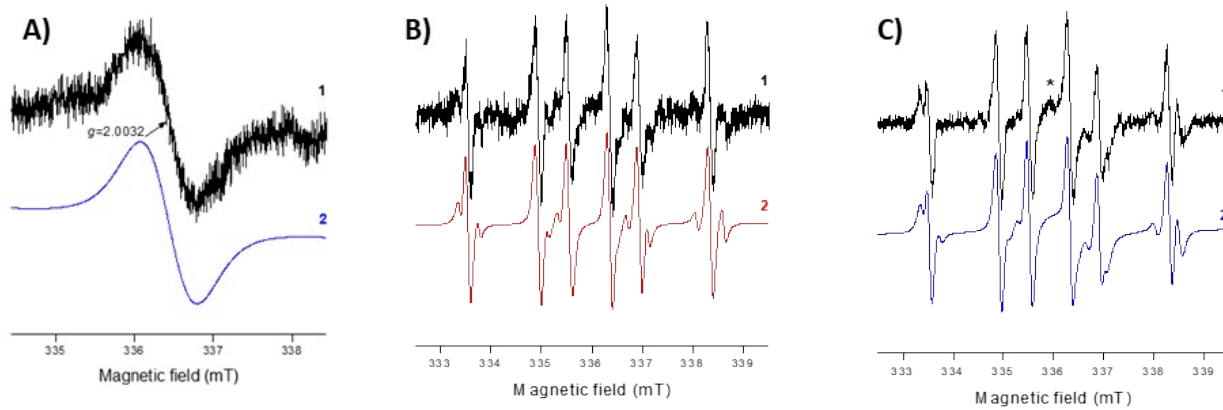


Figure S15: The normalized experimental (1) and simulated (2) EPR spectra obtained upon continuous in situ LED@400 nm exposure in chloroform under irradiation for (A) PBPzn, (B) PBP with DMPO and (C) PBPzn with DMPO.

Effect of the addition of MDEA

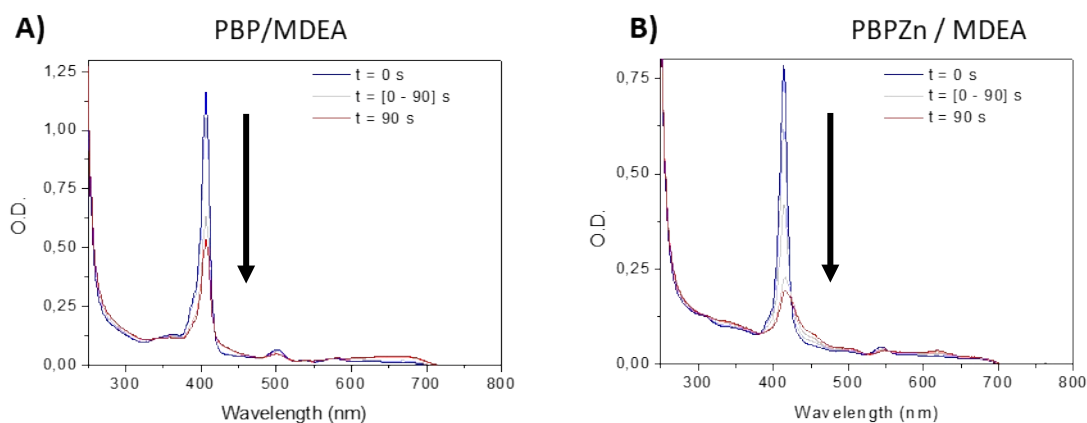


Figure S16 : Steady state photolysis of A) **PBP/MDEA** and B) **PBPZn/MDEA** systems under air after LED@405 nm exposure. $[PBP] = 2 \times 10^{-6} \text{ mol.L}^{-1}$, $[PBPZn] = 6 \times 10^{-6} \text{ mol.L}^{-1}$, $[MDEA] = 2.8 \times 10^{-2} \text{ mol.L}^{-1}$. Solvent = DCM.

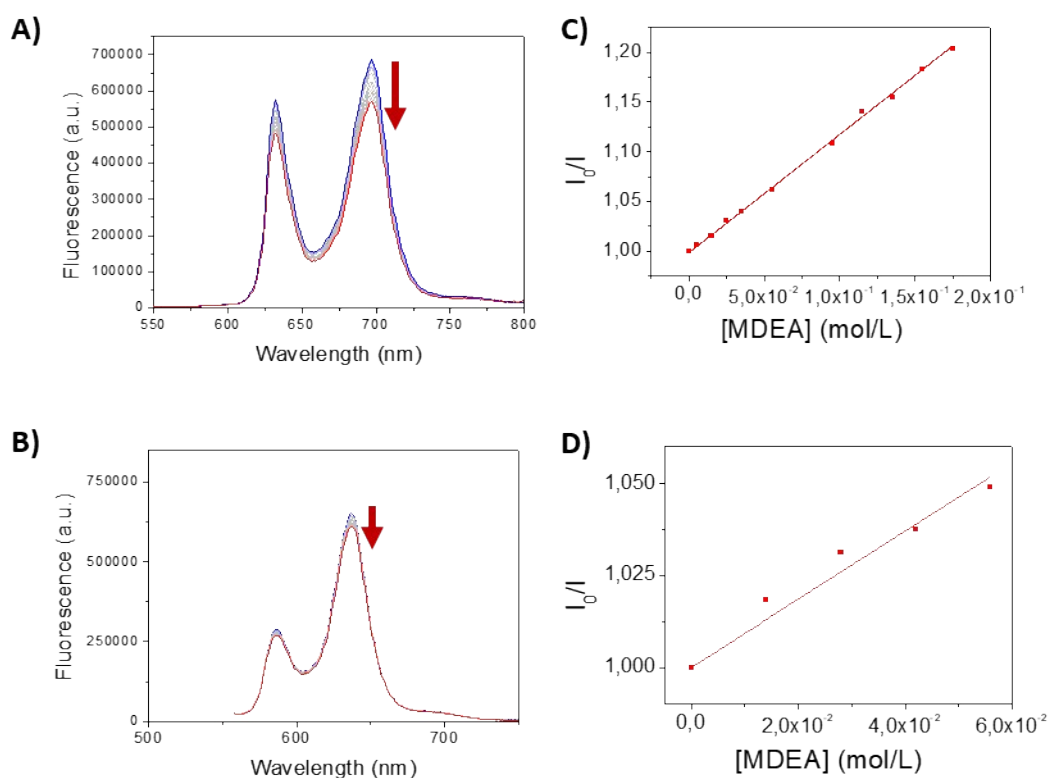


Figure S17 : Quenching of A) **PBP** and B) **PBPZn** fluorescence after a gradual addition of MDEA. $[PBP] = 1.2 \times 10^{-7} \text{ mol.L}^{-1}$, $[PBPZn] = 5.2 \times 10^{-6} \text{ mol.L}^{-1}$ (solvent: THF). Corresponding Stern-Volmer plot for the quenching of the singlet excited state of C) **PBP** ($K_{SV}^{PBP/MDEA} = 1.2 \text{ M}^{-1}$) and D) **PBPZn** ($K_{SV}^{PBPZn/MDEA} = 0.7 \text{ M}^{-1}$) with MDEA.

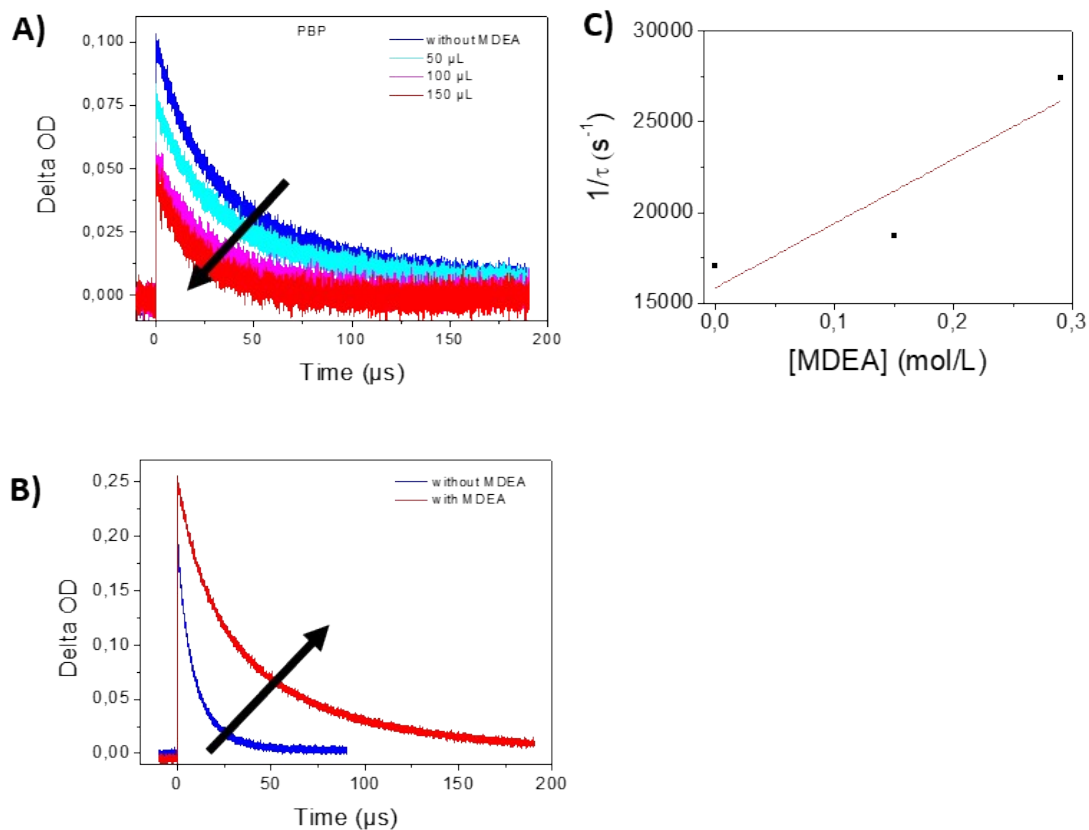


Figure S18 : Decay traces of **A) PBP** and **B) PBPZn** triplet excited state after a laser pulse ($\lambda_{ex} = 385$ nm) with a gradual addition of MDEA. **C)** Corresponding Stern-Volmer plot for the quenching of the triplet excited state of PBP with MDEA. $[PBP] = 1.1 \times 10^{-5}$ mol.L⁻¹, $[PBPZn] = 1.7 \times 10^{-4}$ mol.L⁻¹, $[MDEA] = 8.7$ mol.L⁻¹ in DCM.

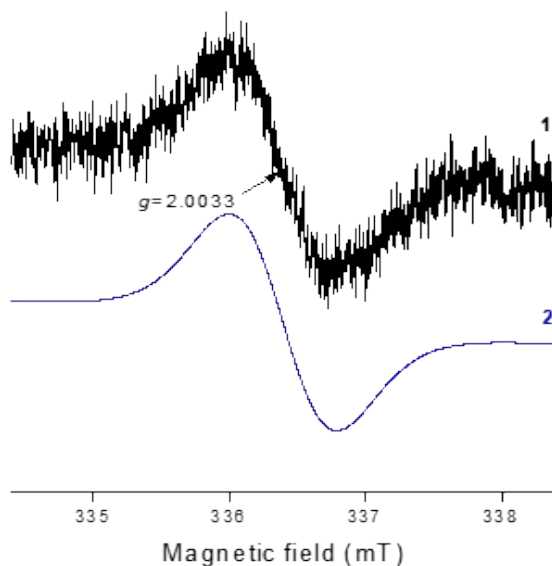


Figure S19: The normalized experimental (1) and simulated (2) EPR spectra obtained upon continuous in situ LED@400 nm exposure of PBPZn/MDEA in chloroform and under argon.

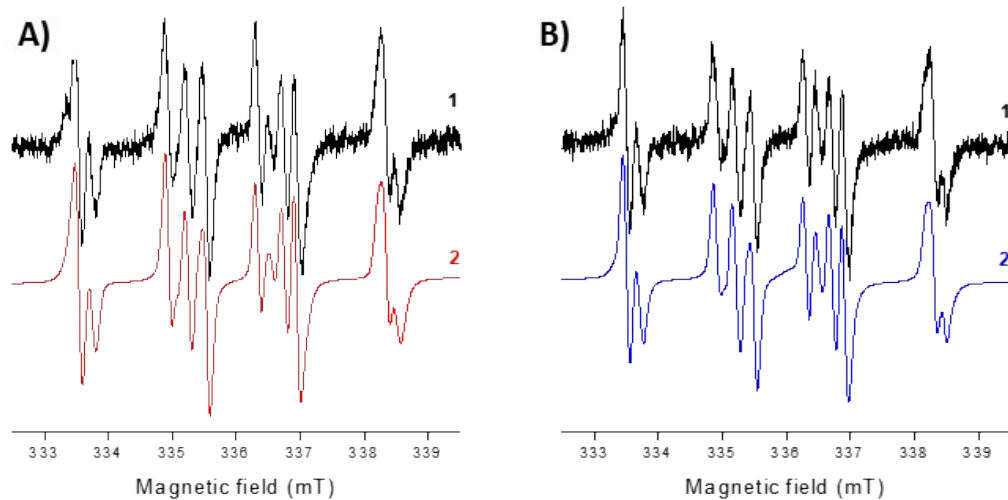


Figure S20 : The normalized experimental (1) and simulated (2) EPR spectra obtained upon continuous in situ LED@400 nm exposure of porphyrin derivatives in chloroform under argon in the presence DMPO spin trapping agent and MDEA for **A) PBP** and **B) PBPZn**.

Effect of the addition of Iod

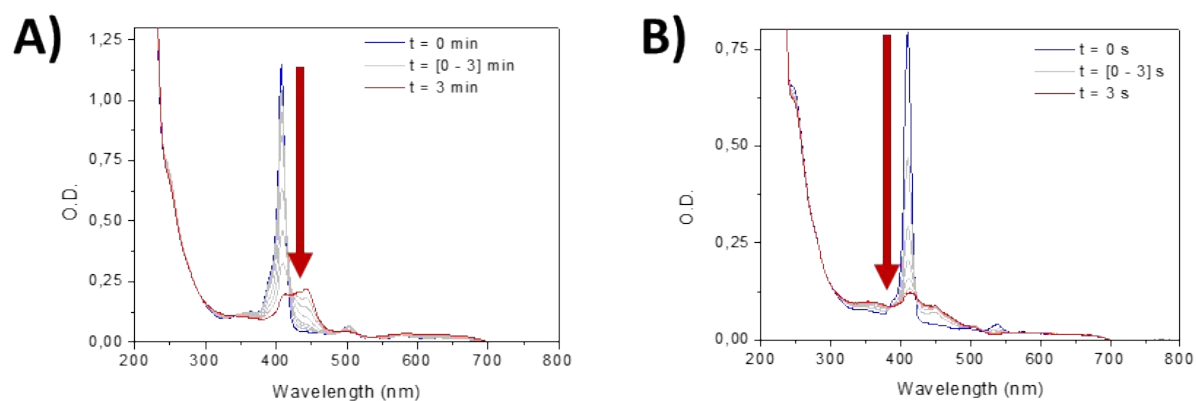


Figure S21: Steady state photolysis of **A) PBP/Iod** and **B) PBPZn/Iod** systems under air after LED@405 nm exposure. $[PBP] = 2 \times 10^{-6} \text{ mol.L}^{-1}$, $[PBPZn] = 6 \times 10^{-6} \text{ mol.L}^{-1}$, $[Iod] = 2.9 \times 10^{-5} \text{ mol.L}^{-1}$. Solvent = DCM

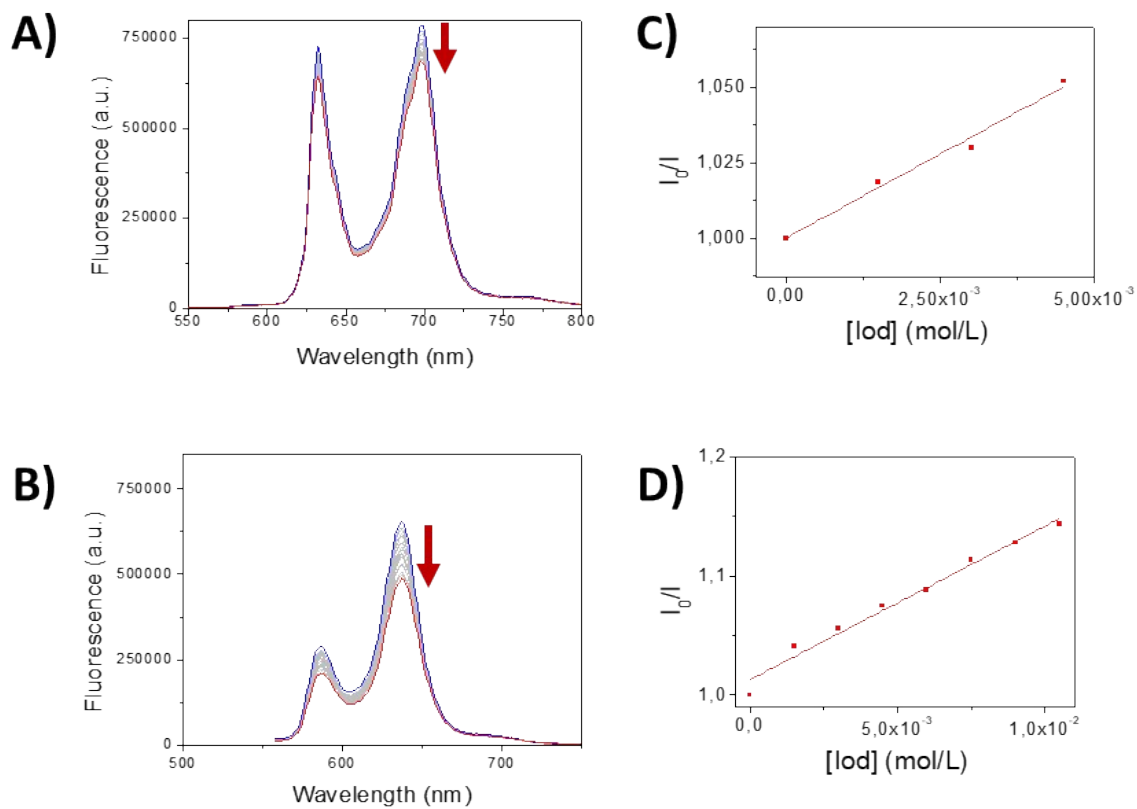


Figure S22: Quenching of A) PBP and B) PBPZn fluorescence after a gradual addition of Iod. $[PBP] = 1.2 \times 10^{-7} \text{ mol.L}^{-1}$, $[PBPZn] = 5.2 \times 10^{-6} \text{ mol.L}^{-1}$ (solvent = THF). Corresponding Stern-Volmer plot for the quenching of the singlet excited state of C) PBP ($K_{SV}^{PBP/Iod} = 11 \text{ M}^{-1}$) and D) PBPZn ($K_{SV}^{PBPZn/Iod} = 13 \text{ M}^{-1}$) with the addition of Iod.

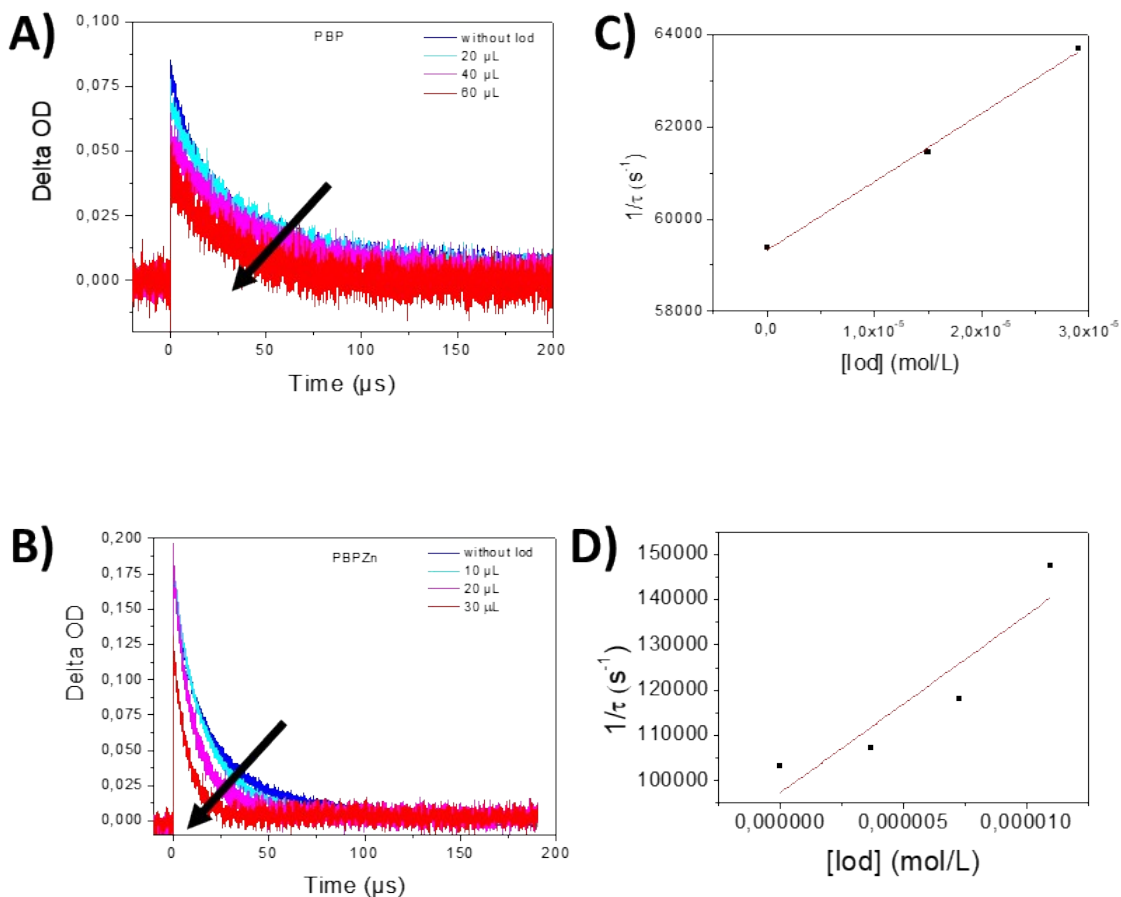


Figure S23: Decay traces of A) **PBP** and B) **PBPZn** triplet state after a laser pulse ($\lambda_{ex} = 385$ nm) with a gradual addition of Iod. Corresponding Stern-Volmer plot for the quenching of the triplet excited state of C) **PBP** and D) **PBPZn** with the addition of Iod. $[PBP] = 1.1 \times 10^{-5}$ mol.L⁻¹, $[PBPZn] = 1.7 \times 10^{-4}$ mol.L⁻¹ in DCM.

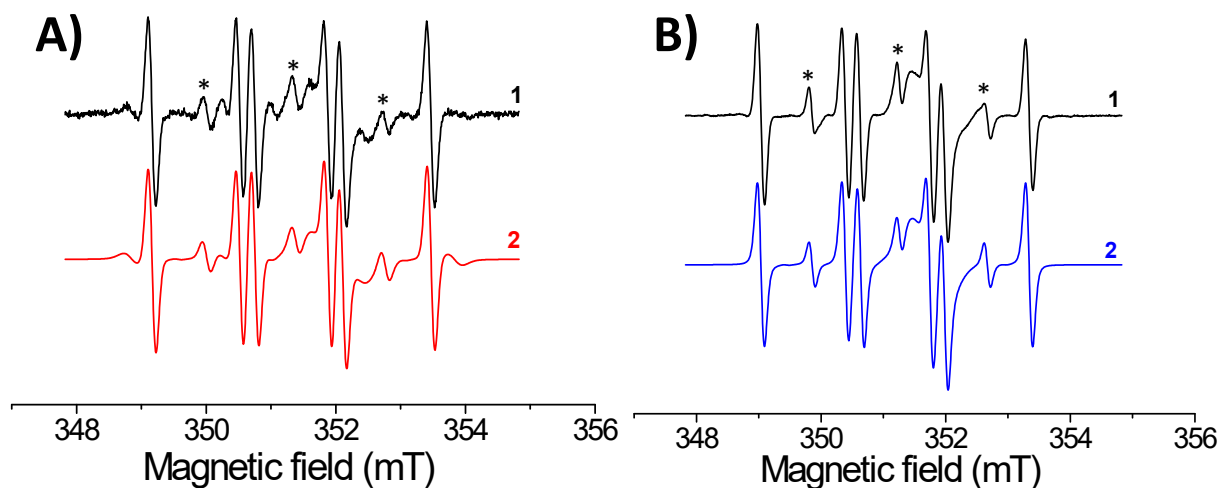


Figure S24: The normalized experimental (1) and simulated (2) EPR spectra obtained post 120-s LED@405 nm exposure of (A) **PBP** and (B) **PBPZn** in chloroform under argon in the presence DMPO spin trapping agent and Iod. (* denote the artefactual triplet lines resulting from double addition of MePh radical on DMPO following a mechanism similar to that detailed in Figure S32 with thiyl radicals).

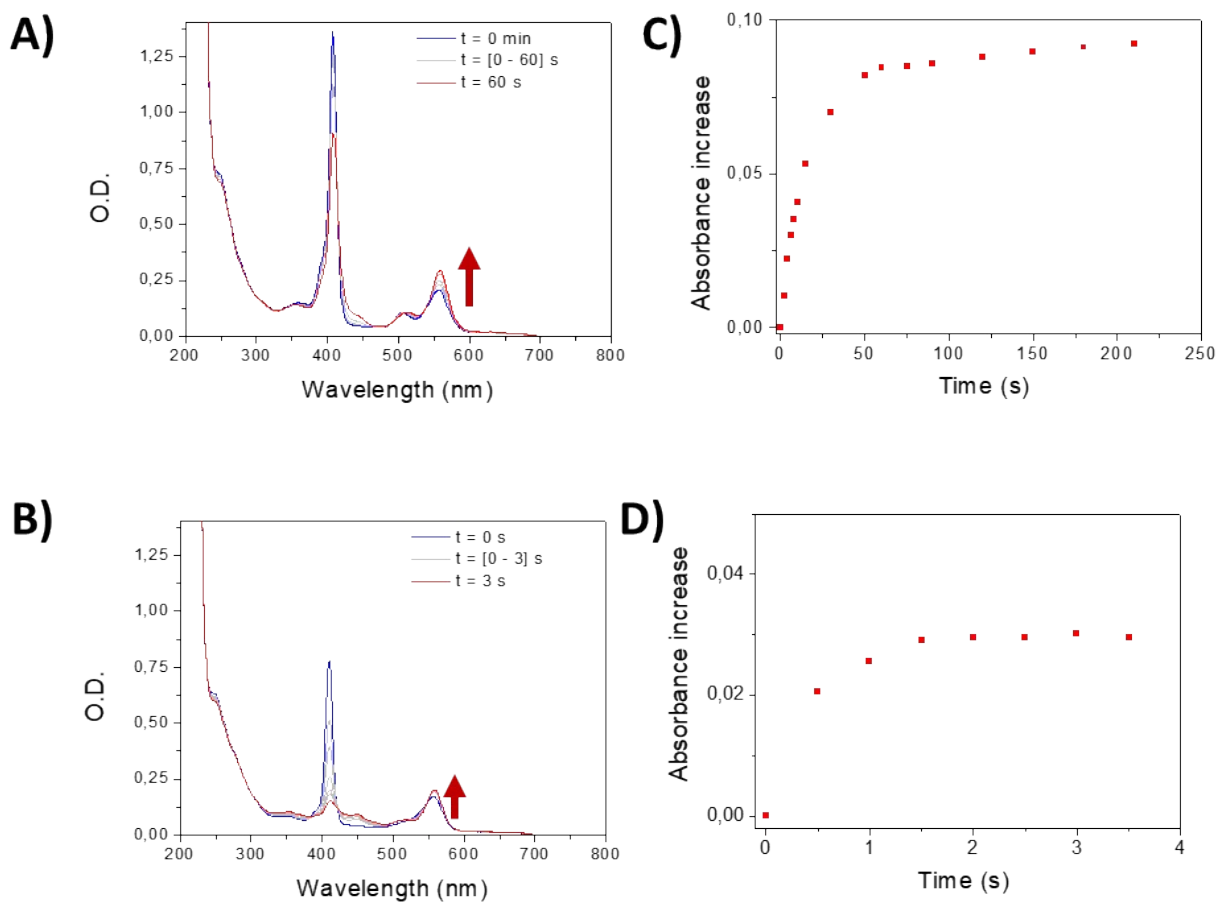


Figure S25: Steady-state photolysis of **A) PBP/iodine/rhodamine B** and **B) PBPZn/iodine/rhodamine B** after irradiation by LED@405 nm under air conditions. Absorbance increase at 570 nm along time for **C) PBP** and **D) PBPZn**. $[PBP] = 2 \times 10^{-6} \text{ mol.L}^{-1}$, $[PBPZn] = 6 \times 10^{-6} \text{ mol.L}^{-1}$, $[Iod] = 2.9 \times 10^{-5} \text{ mol.L}^{-1}$, $[RhB] = 2.4 \times 10^{-5} \text{ mol.L}^{-1}$.

Effect of the addition of cysteamine

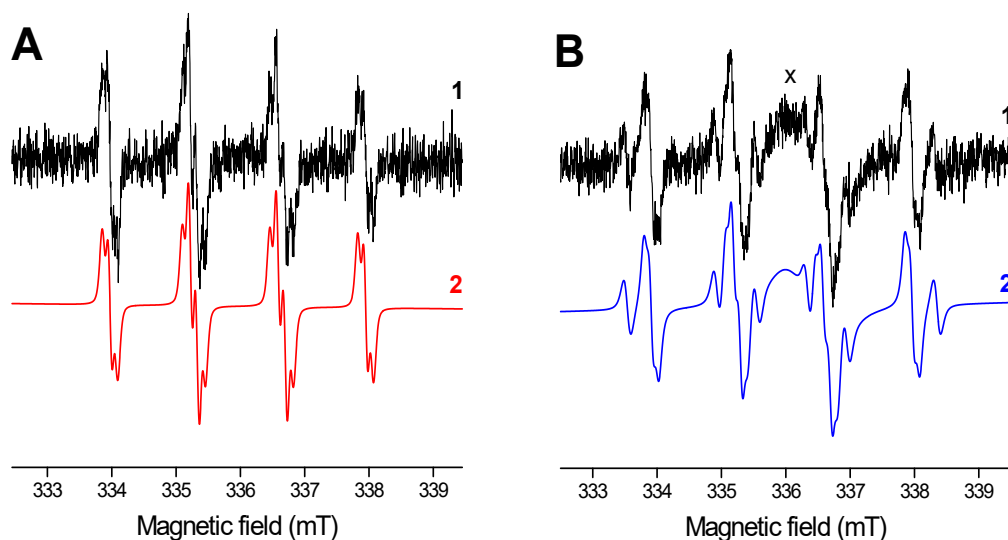


Figure S26: The normalized experimental (1) and simulated (2) EPR spectra obtained upon continuous *in situ* LED@400 nm exposure of (A) **PBP** and (B) **PBPZn** in chloroform and under argon in the presence DMPO spin trapping agent and cysteamine: X denotes the broad signal assigned to $PBPZn^{*+}$.

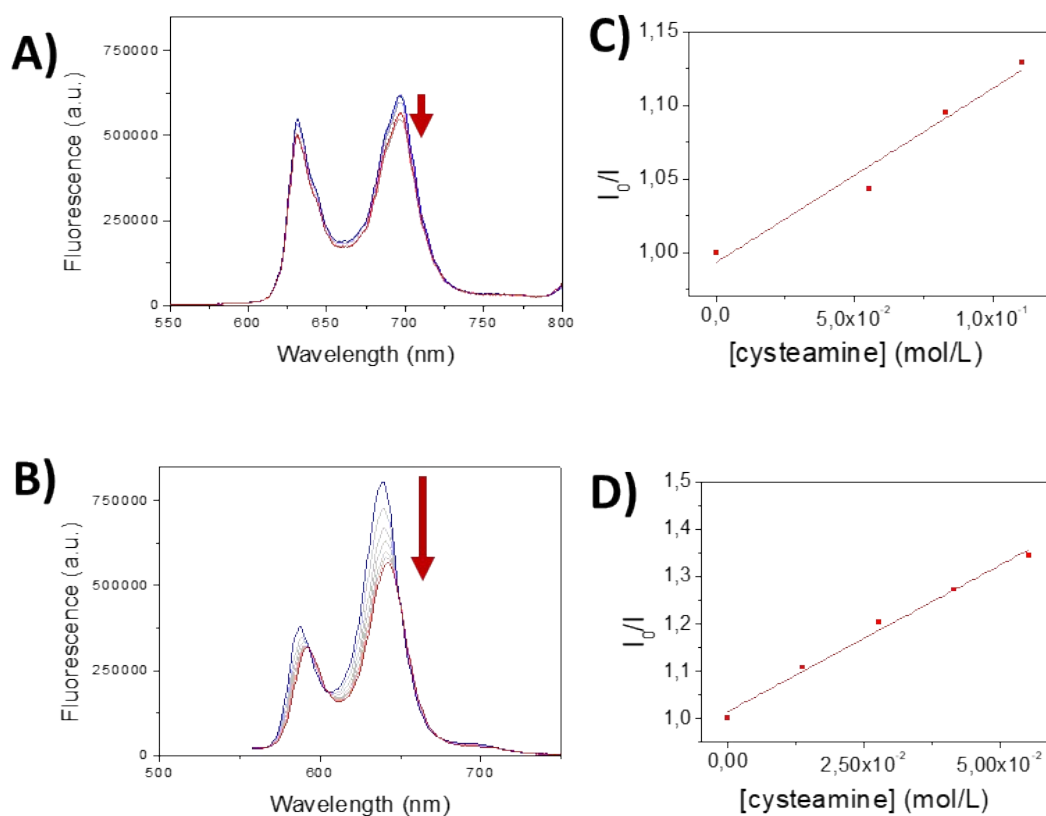


Figure S27: Quenching of A) **PBP** and B) **PBPZn** fluorescence after a gradual addition of cysteamine. $[PBP] = 1.2 \times 10^{-7} \text{ mol.L}^{-1}$, $[PBPZn] = 5.2 \times 10^{-6} \text{ mol.L}^{-1}$ (solvent = THF). Corresponding Stern-Volmer plot for the quenching of the singlet excited state of C) **PBP** ($K_{SV}^{PBP/cysteamine} = 1.2 \text{ M}^{-1}$) and D) **PBPZn** ($K_{SV}^{PBPZn/cysteamine} = 6.2 \text{ M}^{-1}$).

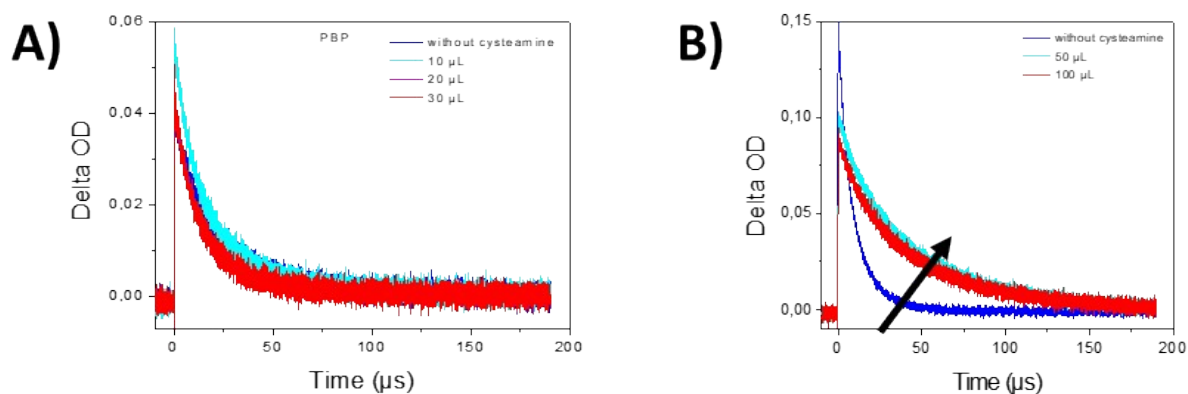


Figure S28: Decay traces of A) **PBP** and B) **PBPZn** triplet state after a laser pulse ($\lambda_{ex} = 385 \text{ nm}$) with a gradual increase of the cysteamine concentration. $[\text{PBP}] = 1.1 \times 10^{-5} \text{ mol.L}^{-1}$, $[\text{PBPZn}] = 1.7 \times 10^{-4} \text{ mol.L}^{-1}$ in DCM.

Effect of the addition of *N*-acetylcysteine

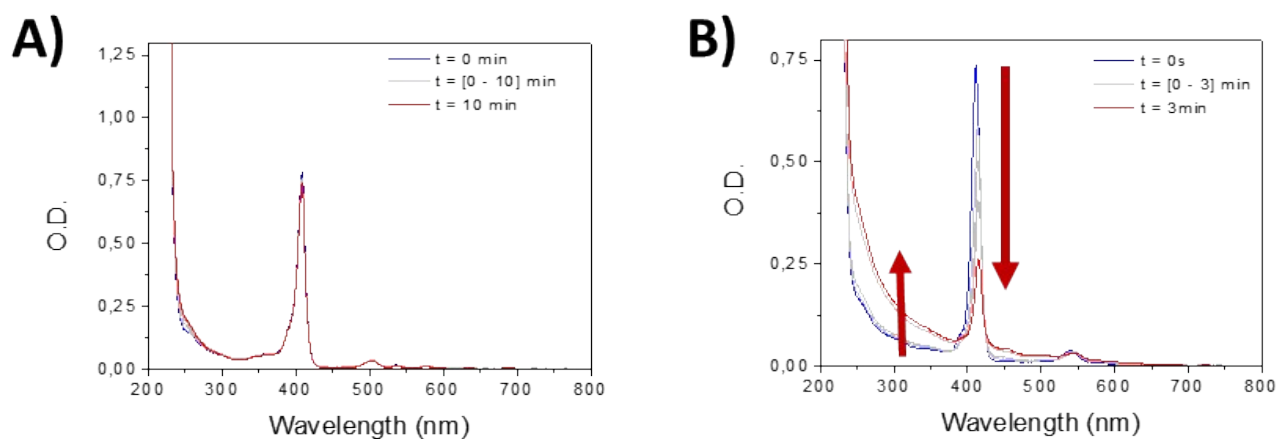


Figure S29: Steady state photolysis of A) **PBP**/*N*-acetylcysteine and B) **PBPZn**/*N*-acetylcysteine systems under air after LED@405 nm exposure. $[\text{PBP}] = 2 \times 10^{-6} \text{ mol.L}^{-1}$, $[\text{PBPZn}] = 6 \times 10^{-6} \text{ mol.L}^{-1}$, $[\text{N-acetylcysteine}] = 1.1 \times 10^{-4} \text{ mol.L}^{-1}$. Solvent = DCM.

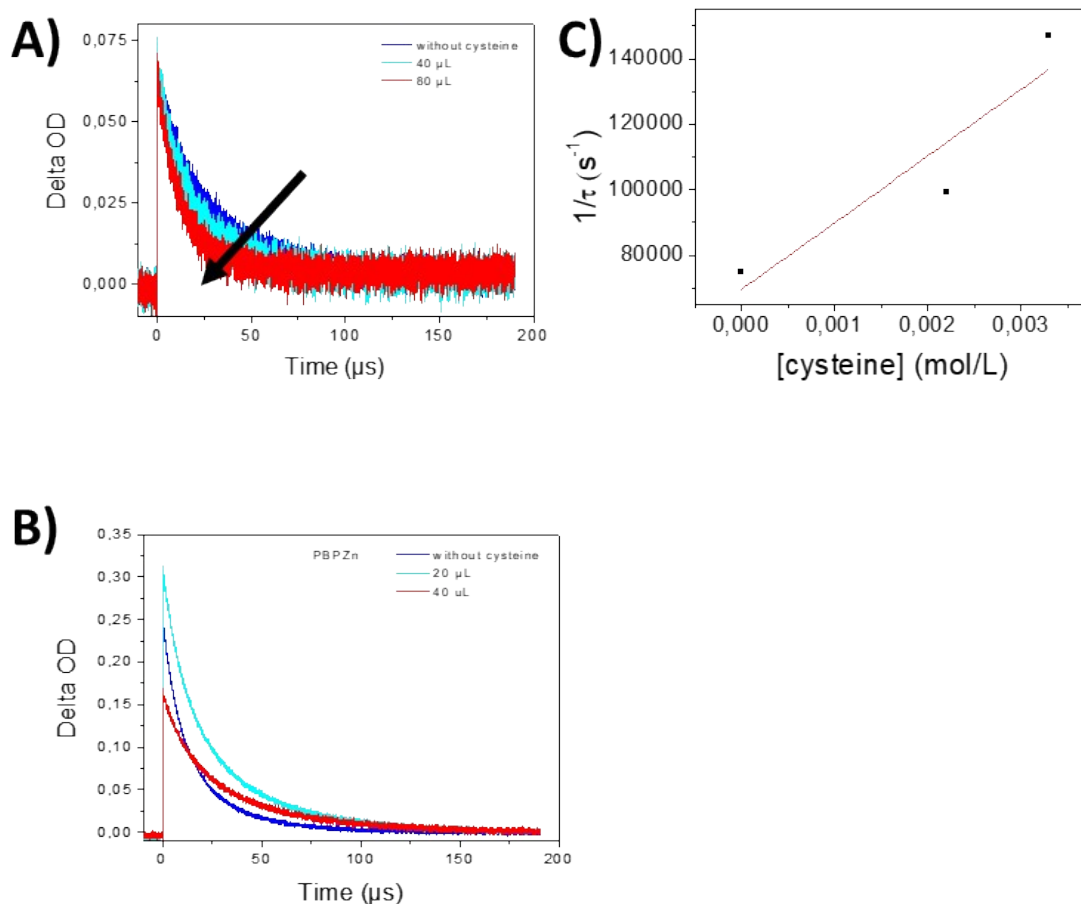


Figure S30: Decay traces of A) **PBP** and B) **PBPZn** triplet state after laser pulses ($\lambda_{ex} = 385 \text{ nm}$) with a gradual addition of *N*-acetylcysteine. Corresponding Stern-Volmer plot for the quenching of the triplet excited state of C) **PBP** with *N*-acetylcysteine. $[\text{PBP}] = 1.1 \times 10^{-5} \text{ mol.L}^{-1}$, $[\text{PBPZn}] = 1.7 \times 10^{-4} \text{ mol.L}^{-1}$ in DCM.

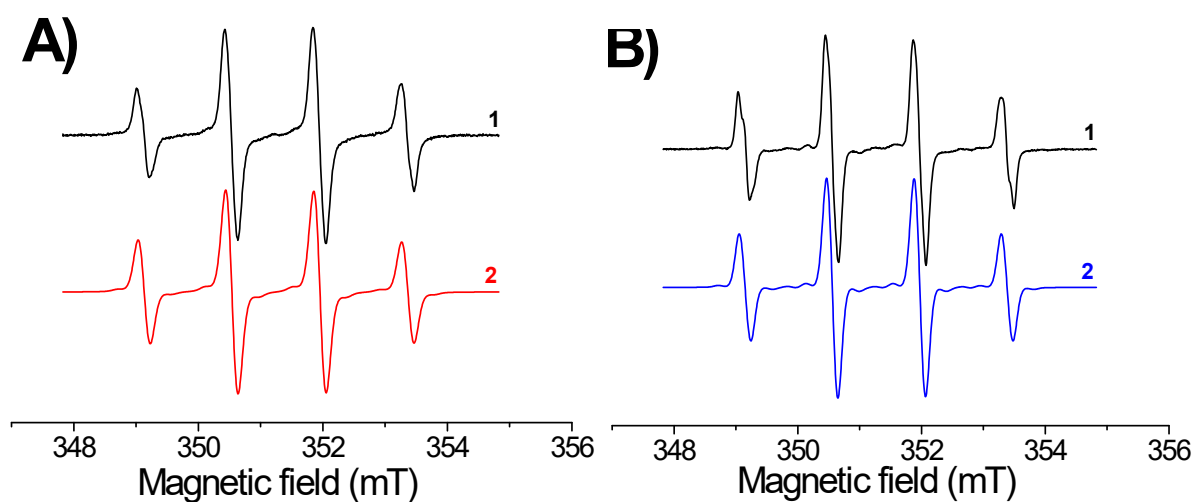


Figure S31: The normalized experimental (1) and simulated (2) EPR spectra obtained upon continuous in situ LED@405 nm exposure of (A) **PBP** and (B) **PBPZn** in chloroform and under argon in the presence of DMPO spin trapping agent and *N*-acetylcysteine.

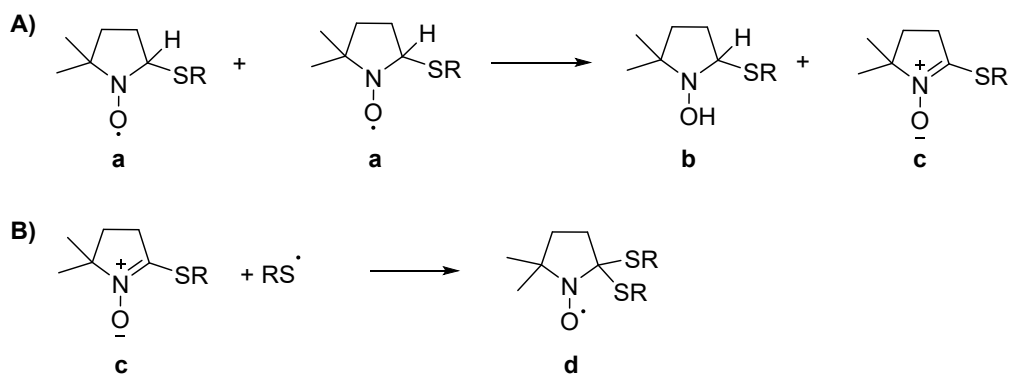


Figure S32: A) Dismutation reaction between two DMPO-SR adduct **a** leading to the formation of hydroxylamine **b** and nitrene **c** by redox reaction. B) Reaction between nitrene **c** and thiyl radical leading to nitroxide **d**.

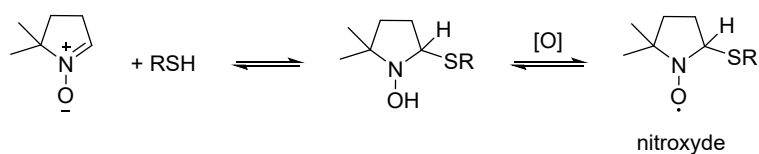


Figure S33: Forrester-Hepburn mechanism

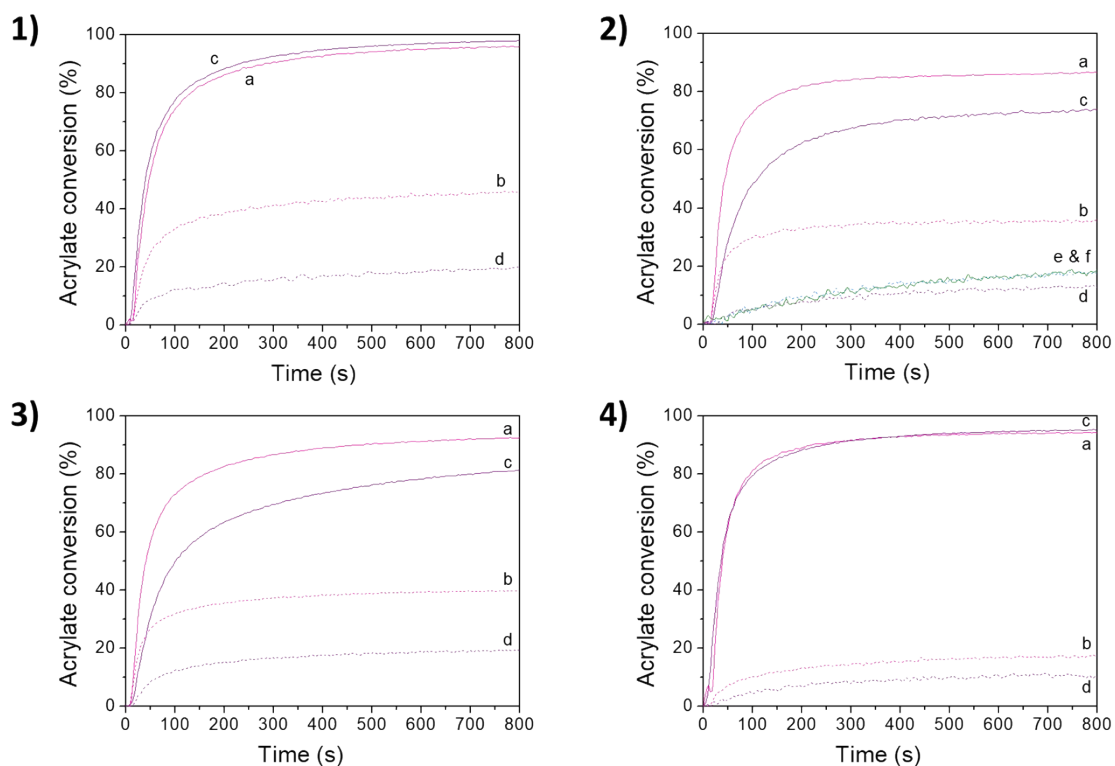


Figure S34: Polymerization profiles (acrylate function conversion vs. irradiation time) for SOA in laminate (solid line) and under air (dash line) in the presence of 1) BP/MDEA (0.5%/2% w/w), 2) BP/Iod (0.5%/2% w/w), 3) BP/cysteamine (0.5%/1% w/w), 4) BP/N-acetylcysteine (0.5%/2% w/w) upon irradiation of (a) LED@385 nm in laminate, (b) LED@385 nm under air, (c) LED@405 nm in laminate, (d) LED@405 nm under air, (e) LED@505 nm under air and (f) LED@530 nm in laminate.

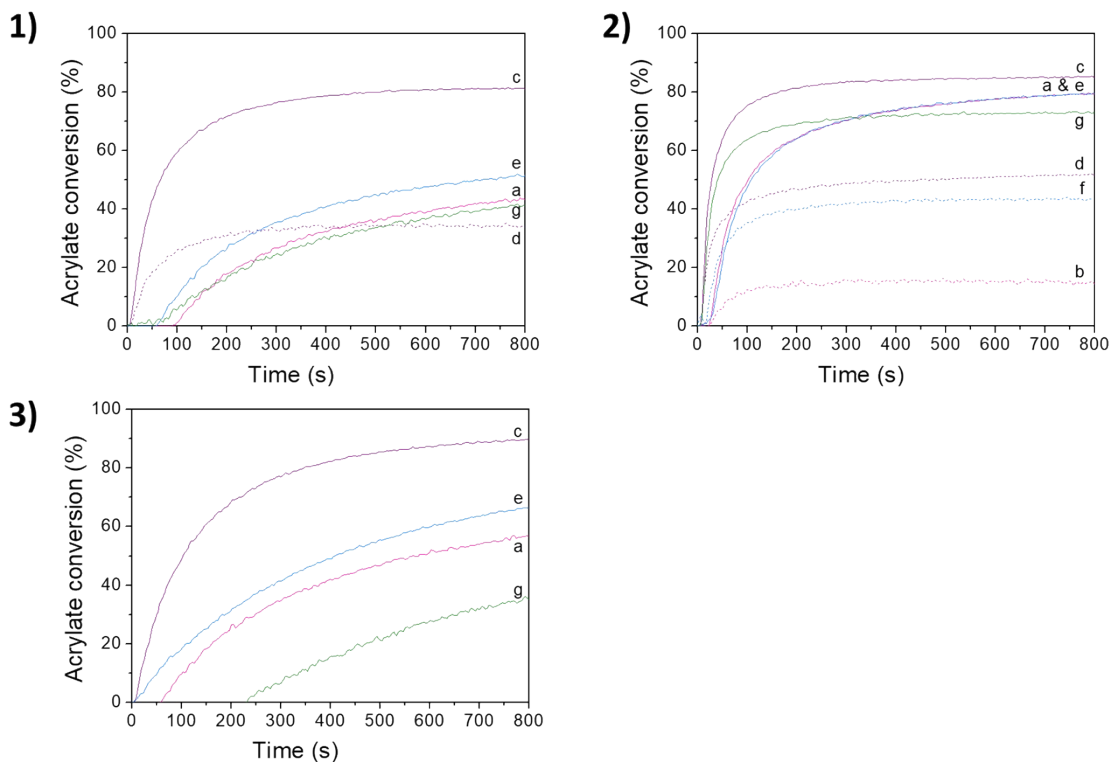


Figure S35: Polymerization profiles (acrylate function conversion vs. irradiation time) for SOA in laminate (solid line) and under air (dash line) in the presence of 1) CQ/MDEA (0.5%/2% w/w), 2) CQ/Iod (0.5%/2% w/w), 3) BP/N-acetylcysteine (0.5%/2% w/w) upon irradiation with (a) LED@385 nm in laminate, (b) LED@385 nm under air, (c) LED@405 nm in laminate, (d) LED@405 nm under air, (e) LED@505 nm in laminate, (d) LED@505 nm under air, (f) LED@530 nm in laminate and (g) LED@530 nm under air.

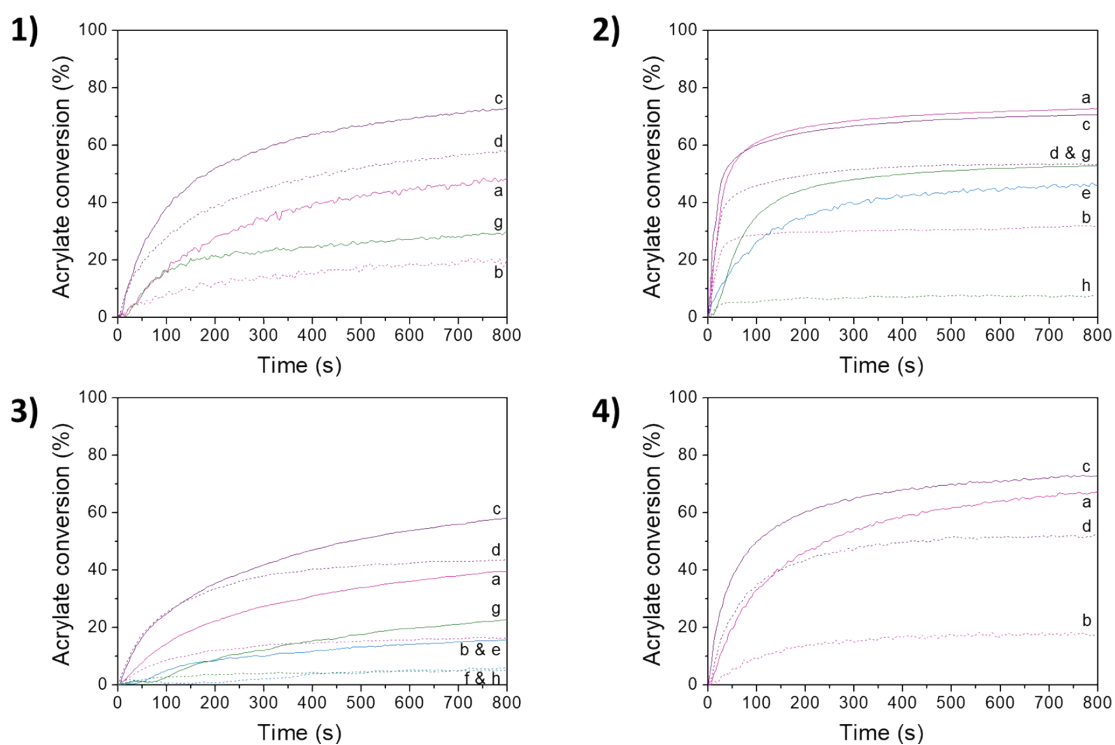


Figure S36: Polymerization profiles (acrylate conversion vs. irradiation time) for SOA in laminate (solid line) and under air (dash line) in the presence of **1) PBP/MDEA** (0.5%/2% w/w), **2) PBP/Iod** (0.5%/2% w/w), **3) PBP/cysteamine** (0.5%/1% w/w) and **4) PBP/N-acetylcysteine** (0.5%/2% w/w) upon irradiation with (a) LED@385 nm in laminate, (b) LED@385 nm under air, (c) LED@405 nm in laminate, (d) LED@405 nm under air, (e) LED@505 nm in laminate, (d) LED@505 nm under air, (f) LED@530 nm in laminate and (g) LED@530 nm under air.

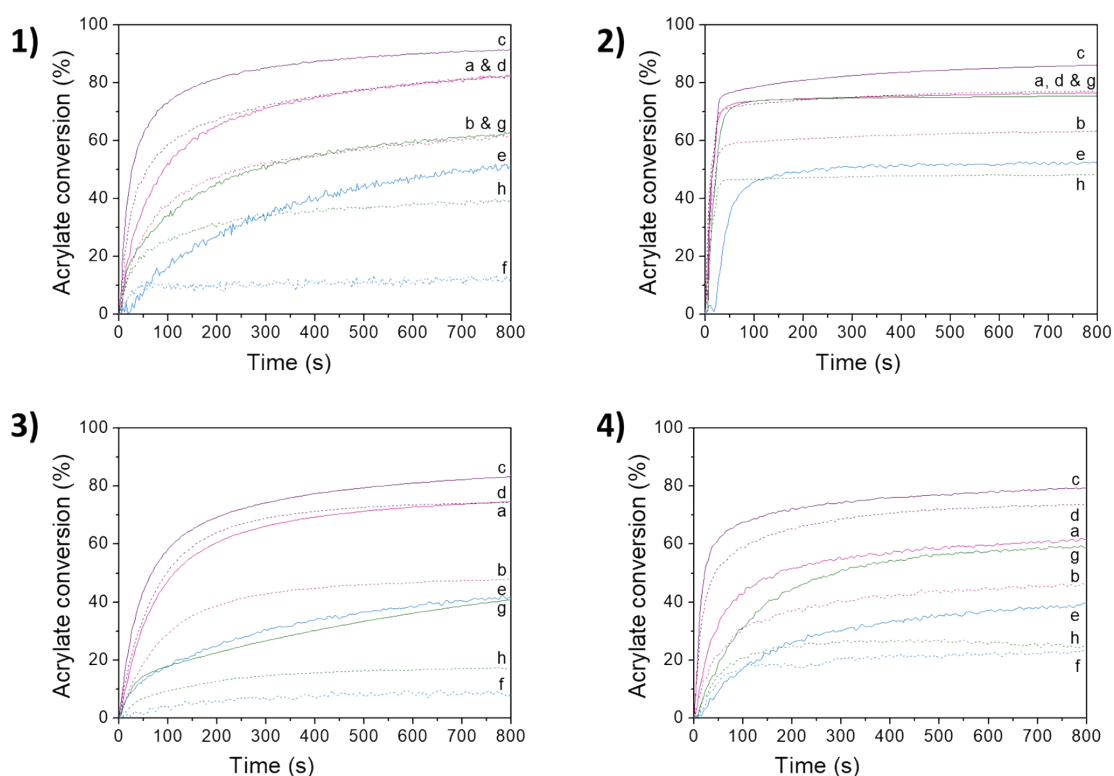


Figure S37: Polymerization profiles (acrylate function conversion vs. irradiation time) for SOA in laminate (solid line) and under air (dash line) in the presence of **1) PBPZn/MDEA** (0.5%/2% w/w), **2) PBPZn/Iod** (0.5%/2% w/w), **3) PBPZn/cysteamine** (0.5%/1% w/w) and **4) PBPZn/N-acetylcysteine** (0.5%/2% w/w) upon irradiation with (a) LED@385 nm in laminate, (b) LED@385 nm under air, (c) LED@405 nm in laminate, (d) LED@405 nm under air, (e) LED@505 nm in laminate, (d) LED@505 nm under air, (f) LED@530 nm in laminate and (g) LED@530 nm under air.



Figure S38: Optical image of the PBPZn-based pellet